Yap Promotes Epithelial Cell Proliferation and Epithelium-derived Innate Cytokine Expression via the NF-κb Pathway in Chronic Rhinosinusitis With Nasal Polyps

Huiyi Deng
Third Affiliated Hospital of Sun Yat-Sen University Department of Otorhinolaryngology Head and Neck Surgery https://orcid.org/0000-0001-9046-5351
Meijiao Li
Third Affiliated Hospital of Sun Yat-Sen University
Rui. Zheng
Third Affiliated Hospital of Sun Yat-Sen University
Huijun Qiu
Third Affiliated Hospital of Sun Yat-Sen University
Tian Yuan
Third Affiliated Hospital of Sun Yat-Sen University
Weihao Wang
Third Affiliated Hospital of Sun Yat-Sen University
Zhuanggui Chen
Third Affiliated Hospital of Sun Yat-Sen University
Qintai Yang
Third Affiliated Hospital of Sun Yat-Sen University
Zijie Long
Third Affiliated Hospital of Sun Yat-Sen University
Xuekun Huang (xuekunhuang@163.com)
Third Affiliated Hospital of Sun Yat-Sen University

Research

Keywords: NF-κB signaling pathway, Yes-associated protein, cell cycle progression, cell proliferation, nasal polyps

Posted Date: June 22nd, 2020

DOI: https://doi.org/10.21203/rs.3.rs-36082/v1

Abstract

Objectives: The hippo-yes-associated protein (YAP) pathway plays an important role in epithelial cell proliferation and inflammation in chronic rhinosinusitis with nasal polyps (CRSwNP). However, the underlying mechanisms remain unclear. This study intends to investigate the role of YAP and the nuclear factor kappa-B (NF-κB) signalling pathway in nasal epithelial cell proliferation and the expression of epithelium-derived cytokines in CRSwNP.

Methods: The expression levels of YAP, TEAD1, Ki-67, and NF-κB in sinonasal mucosa, primary nasal epithelial cells (NPECs), and human nasal epithelial RPMI 2650 cells were detected by RT-qPCR and immunoblotting. NPECs were cultured and treated with verteporfin (VP), a selective YAP inhibitor, YAP shRNA or BAY 11-7082, a small molecule inhibitor of NF-κB. The relationship between cell proliferation and hippo pathway activity was explored using a cell counting kit-8 (CCK-8) assay, 5(6)-carboxyfluorescein diacetate succinimidyl ester (CFSE) labelling and colony formation assay. The cell cycle and apoptosis were examined through flow cytometry (FCM) assay. The epithelium-derived cytokines including interleukin (IL-) 33, IL-25 and thymic stromal lymphopoietin(TSLP) were detected by RT-qPCR.

Results: The hippo pathway effector YAP, Ki-67, p65 NF-κB, and cyclin D1were significantly increased in CRSwNP compared with control mucosa; which was accompanied by overexpression of interleukin (IL)-33, IL-25, and thymic stromal lymphopoieth (TSLP). Pharmaceutical inhibition of YAP by VP suppressed cell proliferation of RPMI 2650 cells by blocking cell cycle progression at G0/G1 without inducing obvious cell apoptosis. Furthermore, lentiviral transfection-mediated knockdown of hippo pathway activity reduced the expression of IL-33,,IL-25, TSLP as well as p65 NF-κB in RPMI 2650 cells. Downregulation of NF-κB pathway with BAY 11-7082 in NPECs could decrease the mRNA level of TSLP, IL-33 and IL-25 accordingly.

Conclusions: Inhibition of hippo pathway suppressednasal epithelial cell proliferation and declined the expression of epithelium-derived cytokines IL-33 and IL-25 and TSLP expression via the NF-κB signalling pathway in NPECs.

1 Introduction

Chronic rhinosinusitis (CRS), with an estimated prevalence of 8% in China (Shi et al., 2015), is defined as chronic inflammation of the nose and the paranasal sinuses, and is characterised by persistent symptoms and typical features at nasal endoscopy and CT scan (Hupin et al., 2014; Stevens et al., 2015). CRS has typically been divided into CRS with nasal polyps (CRSwNP) and CRS without nasal polyps (CRSsNP) based on the presence or absence of polyps under endoscopic examination (W. J. Fokkens et al., 2012). CRSwNP has been typically characterised by epithelial remodelling (Mjosberg et al., 2011; Yan et al., 2013), manifested as abnormal epithelial proliferation, frequent epithelial damage, basal cell proliferation, and a thickened sub-epithelial basement membrane with a reduced number of vessels and

glands but virtually no neuronal structure, goblet cell hyperplasia, or increased extracellular matrix deposition (Watelet et al., 2006; Van Bruaene et al., 2012). Physiologically, the nasal epithelium not only serves as a mechanical barrier through the formation of strong mechanical cohesion by apical (tight and adherens) junctions to protect against environmental factors, microorganisms, and toxins, but also participates in both innate and adaptive immune responses by secreting a large array of antimicrobial host defence molecules (Li et al., 2014).

The hippo-yes-associated protein (YAP) signalling pathway has been indicated to play a critical role in the self-renewal and expansion of stem cells and tissue-specific progenitor cells, and in tissue regeneration and organ size (Johnson, 2019). In mammals, activation of MST1/2 leads to phosphorylation and activation of LATS1/2. YAP and transcriptional coactivator with PDZ-binding motif (TAZ) are phosphorylated by LATS1/2 on multiple sites, resulting in interaction with 14-3-3 and cytoplasmic retention; YAP/TAZ phosphorylation also leads to YAP/TAZ polyubiquitination and degradation. However, when hippo signalling is inactivated, YAP/TAZ enter the nucleus, competes with VGLL4 for the TEAD family of proteins, and recruits other factors to induce gene transcription associated with cell proliferation and differentiation (Halder and Johnson, 2011; Zhao et al., 2011; Yu et al., 2015). YAP has been implicated in airway epithelial cell proliferation and differentiation. For example, YAP is necessary for regular branching morphogenesis and epithelial cell proliferation and differentiation in the developing lung (J. E. Mahoney et al., 2014; C. Lin et al., 2017). In addition, TAZ, a YAP paralog, is vital to normal alveolarisation in mice. When TAZ is deleted, mice have enlarged abnormal alveoli as in human pulmonary emphysema (Mitani et al., 2009). Similarly, deletion of MST1/2 in mice results in increased nuclear YAP, which leads to epithelial hyperplasia and abnormal differentiation of airway epithelial cells (Lange et al., 2015). Furthermore, elevated YAP expression and activity in airway basal stem cells leads to epithelial hyperplasia and inhibits terminal epithelial cell differentiation (Mahoney et al., 2014; Zhao et al., 2014). Recently, we showed that abnormal expression of the hippo-YAP pathway contributed to epithelial proliferation and remodelling in CRSwNP. YAP activity is highly related to epithelia cell proliferation during the pathogenesis of CRSwNP and was positively correlated with the VAS score, Lund-Mackay CT score, and Lund-Kennedy endoscopic score in patients with CRSwNP clinically (Deng et al., 2019). However, the precise mechanisms of cell proliferation, tissue remodelling, and epithelial inflammation are still unclear.

The nuclear factor-kappa B (NF-κB) pathway is thought to play a fundamental role in the regulation and production of pro-inflammatory cytokines and tissue remodelling in nasal polyps NF-κB is a key pro-inflammatory nuclear transcriptional heterodimer consisting of p50 and p65 subunits. When activated, NF-κB translocates to the nucleus where the active p65 subunit induces the transcription of cytokines, chemokines, and adhesion molecules. Several studies have demonstrated a relationship between CRSwNP and the NF-κB pathway. (Chen et al., 2018; Jung et al., 2019). Chen et al. found that interleukin (IL)-17A upregulated the expression of matrix metalloproteinase (MMP)-9 via the NF-κB pathway in nasal epithelial cells (Chen et al., 2018). Jung et al. showed that p65 NF-κB and NF-κB-related inflammatory cytokines were expressed in both eosinophilic and non-eosinophilic nasal polyps. This indicates that NF-κB has a pivotal role in the pathogenesis of CRSwNPs in both Caucasians and Asians, which provides a deeper insight into the pathogenesis of CRSwNPs. (Jung et al., 2019). NF-κB pathway is upregulated in

CRSwNP and is related to IL-6 and IL-8 cytokine expression (Xu et al., 2007). Activation of NF-κB contributed to the pathophysiology of CRSwNP by increasing the expression of various cytokines, chemokines, and adhesion molecules associated with p65 (Jung et al., 2019). In addition, Young Hyo Kim suggested that a therapeutic strategy that targets NF-κB in Asian patients with nasal polyps could be established (Kim, 2019).

In this study, we found that abnormal expression of YAP activity related to epithelial proliferation in nasal polyp tissue during the pathogenesis of CRSwNP. In addition, the NF-κB pathway components were increased in CRSwNP tissue and promoted epithelium-derived thymic stromal lymphopoietin (TSLP), IL-25, and IL-33 expression in patients with CRSwNP. The inhibition of YAP-NF-κB may be a therapeutic strategy for reducing epithelial proliferation and epithelium-derived cytokine production in CRSwNP.

2 Material And Methods

2.1 Subjects

Biopsies of patients with nasal polyps (n = 10) and healthy controls (n = 10) were recruited from the Department of Otolaryngology in The Third Affiliated Hospital of Sun Yat-sen University in China. The demographic information of the study patients is shown in Table 1. The diagnoses and classification of CRS were based on the European Academy of Allergy and Clinical Immunology (EAACI) guidelines (EPOS2012) (Fokkens et al., 2012). All NP patients were bilateral with Grade-3 NP which had completely obstructed the nasal cavity. None of the NP patients and controls had a concurrent upper respiratory infection, asthma and other systemic diseases. In addition, any form of glucocorticosteroids or antibiotics within three months were did not be used before the study. Biopsies were obtained during functional endoscopic sinus surgery (FESS). Biopsies of inferior turbinate (IT) mucosa were obtained from the healthy patients, who had no history of CRS and no evidence of sinonasal mucosal inflammation on endoscopy but were undergoing sinonasal surgery for other indications, such as deviation of septum, pituitary tumors, encephaloceles, or repair of cerebrospinal fluid rhinorrhea.

Table 1
Patient characteristics and histopathological evaluation

	Controls	CRSwNP
Sample number	10	10
Average Age (Range)	28 (22–47)	40(19–50)
Gender (Male/Female)	9/5	6/8
Smoking history	2	4
Asthma	0	0
Allergic rhinitis	0	0

Parts of the fresh nasal tissues were used for quantitative reverse transcription-polymerase chain reaction (qRT-PCR) and histological analysis, and some of the tissues were isolated for cell culture.

2.2 Immunohistochemistry in Solid Tissues

Tissue samples were fixed in 10% neutral buffered formalin and embedded in paraffin. Paraffin sections (4 μm) were prepared for each block. Sections were subjected to heat-induced antigen retrieval. Endogenous peroxidase activity was blocked with 0.3% hydrogen peroxide. Nonspecific staining was blocked with 5% bovine serum albumin (Boster Biotechnology). Sections were conducted with specific primary antibodies YAP (1:100, CST, #14074), NF-κB (1:100, Servicebio, GB11142) and cyclin D1(1:100, CST, #14074) as previously reported (Deng H et al., 2019).

2.3 Immunoblotting

Total protein from the treated cells and tissues were extracted by RIPA buffer with the mixture consisting of protease Inhibitor Cocktail (Beyotime, Shanghai, China). Protein was separated by an 8% SDS-PAGE gel and transferred to polyvinylidene difluoride membranes (Millipore, IPVH10100). After blocking with 5% bovine serum albumin (BSA) for 75 minutes, the PVDF membrane was incubated with primary antibodies (YAP Rabbit mAb (1:1000, CST, #14074),, TEAD1 Rabbit mAb (1:1,000, CST, #12292), Anti -Ki67 Rabbit pAb (1:1000, Servicebio, GB11030), NF-κB p65 (D14E12) XP® Rabbit mAb (1:1000, CST, #140748242), Anti-Cyclin D1 antibody (1:1000, Abcam, ab16663), Anti-CDK4 antibody (1:1000, Abcam, ab108357, Phospho-IκBα (Ser32/36) (5A5) Mouse mAb (1:1,000, CST, #9246), IκBα (112B2) Mouse mAb (Carboxy-terminal Antigen, 1:1,000, CST, #9247) and rabbit monoclonal anti-GAPDH antibody (1:3,000, Bioworld, AP0063) at 4 ℃ overnight. After washing for three times, the membrane was incubated with HRP-conjugatedsecondary antibodies for 1 h at room temperature. Finally, enhanced chemiluminescence (Advansta, K-12045-D50) was used to visualize the immunoblot. The intensity of the bands was determined by Image J software. The ratio of each band/GAPDH was considered as the expression level of the target protein.

2.4 RNA Extraction and Real-Time Polymerase Chain Reaction Analysis

The quantitative real-time PCR was performed as previously reported (Deng et al., 2019). All primers used are listed in Table 2. The total RNA (1 μg) of each tissue sample was extracted using RNAiso Plus (TaKaRa, Japan) and reverse-transcribed to cDNA with random hexamer primers and RT-PCR kits (TaKaRa RR047A, Japan). The YAP, IL-25, IL-33 and TSLP were detected. PCR was performed with an ABI 7500 FAST instrument (Foster City, CA, USA) using an SYBR Premix Ex Taq kit (TaKaRa DDR420A, Japan). The relative fold increase of gene expression was calculated using the comparative 2-ΔΔCt method. β2 microglobulin (β2M) was used as the housekeeping gene for normalization.

Table 2
Primer sequences for real time quantitative PCR

Gene name	Primer sequence (5′- 3′)
β_2M	TACACTGAATTCACCCCCAC
	CATCCAATCCAAATGCGGCA
TSLP	CCCAGGCTATTCGGAAACTCA
	ACGCCACAATCCTTGTAATTGTG
IL-33	AGCCTAGATGAGACACCGAATT
	GGTCAGAAGGGATGGTAGGC
IL-25	CCAGGTGGTTGCATTCTTGG
	TGGCTGTAGGTGTGGGTTCC

2.5 Human Nasal Epithelial Cells and RPMI 2650 Culture

Human nasal epithelial cell culture was performed as previously reported (Deng et al., 2019). Fresh specimens from healthy controls and nasal polyp tissues were immediately washed with cold phosphate-buffered saline supplemented by penicillin, streptomycin and amphotericin repeatedly, which were then cut into pieces and digested by Dispase II (Sigma, St. Louis, MO, D4693) dissolved with DMEM/F-12 (Hyclone, SH30023.01) at 4℃ overnight. A single-cell suspension was obtained after digesting with pancreatin at 37℃ for 15 minutes and grinding with 1640 medium (Thermo Scientific) containing 10% fetal bovine serum (FBS). Cells were seeded and cultured with Serum- and BPE-free medium (STEMCELL, #05008) at 37℃ for about 10 days to 80% confluence. These cells were then treated with Verteporfin, Selleck, S1786) for 24 h or BAY 11-7082, a NF-κB small molecule inhibitor, for 24 h. RPMI 2650 (Sigma Aldrich), a nasal epithelial cell line, was cultured in 1640 medium with 10% FBS at 37℃ in an atmosphere of 5% CO2 (Chen et al., 2018).

2.6 Construction of The Lentiviral Interference Vectors and Transfection.

Sequence of the shRNA targeting YAP was designed as follows: 5'-GCCACCAAGCTAGATAAAGAA-3' as described by Rosenbluh, J., et al (Rosenbluh J et al., 2012). Non-silencing shRNA (5'-TTCTCCGAAC GTGTCACGT-3') was synthesized as the negative control (NC shRNA). The shRNA was then ligated into lentiviral interference vector,pHBLV-U6-MCS-CMV-ZsGreen-PGK-PURO. When HEK 293T cells were transfected with the lentiviral packaging plasmids (pSPAX2, pMD2G, and YAP shRNA) using the LipoFiter™ Liposomal Transfection Reagent (Hanbio Biotechnology, Shanghai, China), and the viral particles (YAP shRNA) were collected. Finally, both the lentivirus was extracted and concentrations were verified.

For lentivirus transfection, the RPMI 2650 cells were grown to 50–70% confluency and infected with YAP-shRNA and the control shRNA with polybrene at a concentration of 8 μg/ml. Cells were washed and switched into the complete medium after transfection after 8 h. The fluorescence was used to confirm the successful transfection of YAP-shRNA lentiviral vectors 2 d after transfected. The YAP-shRNA infected cells were detected as GFP-positive cells. Stable cell lines containing YAP-shRNA or NC vector were selected using 2.5 μg/ml puromycin (Beyotime, China).

2.7 Immunofluorescence Staining in Cell Cultures and Confocal Microscopic Imaging

Immunofluorescence staining was performed as previously reported(Deng H et al., 2019). RPMI 2650 cells were cultured on coverslips and treated with VP for 24 h when grown to 80% confluence. After the VP treatment, cells were washed in PBS buffer twice. Next, the treated cells were fixed by 4% paraformaldehyde at room temperature for 10 minutes. Subsequently, cells were treated with 0.1% Triton X-100 for 5 minutes at room temperature to permeabilize cells membranes. After nonspecific blocking, the cells were blocked in TBST and 1% Bovine Serum Albumin at room temperature for 90 minutes, then the cells were incubated with primary antibody (Anti-NFkBp65 Rabbit pAb (1:200, Servicebio, GB11142) overnight at 4℃. Cells were next incubated with secondary antibody (1:500) conjugated with Alexa Fluor 488-conjugated goat anti-rabbit IgG (Life Technologies, GrandIsland, NY, BIOTIUM-20012) for 2 h at 37℃ in dark. Cell nuclei were counterstained with SlowFade Gold antifade reagent with 49, 6-diamidino-2-phenylindole (DAPI) (Thermo Scientific, D1306). The slides were then analyzed with a confocal microscope (Nikon C2, Japan).

2.8 Colony Formation Assay

RPMI 2650 cell lines, shYAP or NC stable cells, and NPECs were seeded and cultured into the six-well plate at a density of 300 cells/well in DMEM containing 10% FBS or with serum-free bronchial epithelial cell growth medium (BEGM) (Lonza, CC-3171) for 24 h. Then, the cells were treated with various concentrations of VP (0,10 μM for RPMI 2650 cell; 0, 2.5 μM for NPECs). After the treatment, the cells were cultured in 5% CO_2, 37 °C for 7 days to allow colony formation. The colonies were fixed by 4% paraformaldehyde at room temperature for 10 minutes. Then dyed with 0.1% crystal violet (Solarbio, China) at room temperature for 15 minutes. Colonies were photographed using BioRad GS-800 Calibrated Densitometer. The colonies and counted by Image J software. The experiment was repeated three times.

2.9 5(6)-carboxyfluorescein Diacetate Succinimidyl Ester (CFSE) Labelling and Flow Cytometry Assay

Primary epithelial cells from nasal polyps (NPECs, 1×10^6 cells/mL) or RPMI 2650 cells were washed twice with PBS and collected. The cells were resuspended in 500μL PBS buffer and stained with 5 μM CFSE (Biolegend, USA, 423801) for 10 minutes at 37℃ in dark. Then cells were treated with 10 volumes of ice-cold culture medium (10% FBS) and were washed with cold PBS buffer twice to remove excess dyes and seeded in 6-well plates for 24 h. Next, the cells were treated with various concentrations of VP

(0, 10, 15, 20 μM or 0, 2.5, 5, 10 μM) for 24 h. After the treatment, the percentage of cell proliferation was analyzed by using flow cytometry (BD, FACSCalibur, USA) to evaluate the CFSE fluorescence intensity. The experiment was done for three times.

2.10 Flow Cytometry Assay of Cell Cycle and Apoptosis

24 h after VP treatment at different concentration (0, 10, 15, 20 μM), RPMI 2650 cells were trypsinized and then centrifuged at 1,500 rpm for 5 minutes, followed by wash in cold PBS twice. Next, 70% cold ethanol was added and cells were fixed for more than 2 h. A total of 250 μl PI/RNase buffer was added and incubated for 30 minutes at RT. Finally, cells analyzed on a flow cytometer (BD Biosciences).

For apoptosis analysis, cells were stained with the Annexin V-FITC/PI apoptosis detection kit (Bestbio, China). The rate of apoptotic cells was analyzed using a dual laser flow cytometer and estimated using the ModFit software (BD Biosciences).

2.11 Cell Counting Kit-8 (CCK8) Assay

Cell viability analysis was measured by Cell Counting Kit-8 (CCK8, Beyotime, Shanghai, China) according to the manufacturer's protocols. NPCEs were harvested and cultured at a density of 2×10^3/well into 96-well. Next, the cells were treated with different concentrations of (Verteporfin, 0, 1.25, 2.5 5, 10, 15, 20, 30, 40 μM, Selleck, S1786). After treatment for 6, 12, 24 and 48 h, respectively, 10 μL of CCK-8 reagent was added to every well and then cultured for 2 h in dark. All experiments were performed for three times. The absorbance analysis was using a microplate reader at 450 nm (Bio-Rad, Hercules, CA, USA).

2.12 Statistical Analysis

All data are presented as means and standard error (mean ± SD) from the indicated number of samples. If not normally distributed, data were expressed as median. In continuous variables, for non-normally distributed data, the Kruskal-Wallis H-test was used to assess significant intergroup variability. Normal data were assessed by one-way ANOVA for multiple comparisons. The Mann-Whitney *U* 2-test was applied for non-normally distributed data or Student's t test was used for unpaired data between two groups analysis. Statistical analysis was performed using IBM SPSS software (SPSS, Inc, Chicago, IL, USA), and GraphPad Prism 6 (GraphPad Software, San Diego, CA, USA). Two-tailed *P* value less than 0.05 indicates as statistical significance.

3 Results

3.1 Aberrant expression of YAP, epithelial cell-derived cytokines, and cyclin D1 in CRSwNP

Firstly, we explored the expression of YAP, the cell proliferation marker Ki-67, and NF-κB in polyp tissues by western blotting analysis. We found that the protein levels of YAP, Ki-67, and NF-κB were significantly increased in nasal polyp tissues compared with healthy nasal tissues (Fig. 1A and B). Since cyclin D1 is

related to cell proliferation (Zhang et al., 2020), we detected the expression of YAP, NF-κB, and cyclin D1 by immunohistochemistry in nasal polyps and normal control tissues. We found that the expression levels of YAP, NF-κB, and cyclin D1 were significantly increased in nasal polyps. Consistently, YAP, NF-κB, and cyclin D1 were mainly upregulated in the epithelium, and low levels were found in the lamina propria in nasal polyps (Fig. 1C). Moreover, to explore the levels of epithelium-derived innate cytokines, we determined the mRNA levels of TSLP, IL-33, and IL-25 by RT-qPCR. The results showed that the mRNA levels of TSLP, IL-33, and IL-25 were significantly upregulated in nasal polyps compared with those of normal control tissues (Fig. 1D). Together, these results indicate that the hippo pathway effector YAP might be involved in epithelium-derived cytokine expression and inflammation via the NF-κB pathway in nasal polyps.

3.2 Inhibition of YAP suppresses the proliferation of RPMI 2650 cells

To investigate the impact of YAP on cell proliferation, different density gradients of verteporfin (VP) were used to treat RPMI 2650 cells. We assessed cell viability at 24 h using a CCK-8 assay. Compared with the control group, a dose-dependent decrease in cell viability was observed in the VP group in (Fig. 2A). As shown in Fig. 2B, the cell morphology changed after VP treatment. We further examined the proliferation of the three VP-treated cell groups (10, 15, and 30 μM) by cell counting. After inhibiting YAP expression in RPMI 2650 cells for 24 and 48 h, we found that there was a significant reduction in cell proliferation (Fig. 2C). The results demonstrated that downregulation of YAP led to suppression of epithelial cell proliferation. Further testing using 5(6)-carboxyfluorescein diacetate succinimidyl ester (CFSE) labelling was performed to confirm the ability of the proliferation inhibition of VP. The results revealed that the proliferation of cells treated with 15 μM and 20 μM VP was greatly reduced (Fig. 2D and E). Colony formation assays also showed much less colony formation in the group treated with 10 μM VP compared with the control group (Fig. 2F and G). Moreover, the western blotting results revealed that VP considerably decreased the expression levels of YAP and TEAD1 in a dose-dependent manner, together with Ki-67 (Fig. 2H). These results indicate that pharmaceutical inhibition of YAP suppressed the proliferation and colony formation ability of RPMI 2650 cells.

3.3 Inhibition of YAP arrests the cell cycle

After RPMI 2650 cells were treated with different concentrations of VP, the effect of YAP on cell cycle progression was analysed by FCM In the 20 μM VP group, we found that 83.81% of cells were in G1 phase and 7.93% were in S phase. In comparison, 86.12% of cells were in G1 phase and 8.58% were in S phase in the 15-μM group, 77.92% of cells were in G1 phase and 11.67% of cells were in S phase in the 5 μM VP group, and 58.87% of cells were in G1 phase and 31.52% of cells were in S phase in the control group (Fig. 3A and B). In addition, we further explored the protein levels of cyclin D1 and cyclin-dependent kinase (CDK) 4, which are involved in cell cycle regulation. Western blot analysis indicated that both

cyclin D1 and CDK4 levels were decreased after VP treatment compared with the untreated group (Fig. 3C).

Furthermore, the apoptosis rate of cells treated with VP was analysed by FACS. The results showed that in RPMI 2650 cells with pharmaceutical inhibition of hippo pathway activity, the apoptosis rate was slightly increased compared with the group without VP treatment. However, the difference between the blank control and the 20-μM VP group was not significant ($P > 0.05$, Fig. 3D). These findings suggest that downregulation of YAP induced G1 phase arrest, resulting in suppression of cell proliferation.

3.4 Inhibition of YAP suppresses NF-κB pathway and epithelium-derived factor expression in RPMI 2650 cells

To further explore whether pharmacological inhibition of hippo pathway activity affects the NF-κB pathway and epithelium-derived factor expression in epithelial cells, we treated RPMI 2650 cells with VP, and knockdown YAP using lentiviral transfection. Western blotting showed that the expression of NF-κB decreased in RPMI 2650 cells treated with VP in a dose-dependent manner (Fig. 4A). Immunofluorescence analysis confirmed the expression of NF-κB in the epithelial cells of nasal polyps treated with 20 μM VP (Fig. 4B). Previous study shows that epithelial cells produces epithelium-derived factors (Mjosberg et al., 2011), and we found that VP significantly decreased the mRNA levels of IL-33, TSLP, and IL-25 in a dose-dependent fashion (Fig. 4D–F). As expected, both Ki-67 and TEAD1 were significantly decreased after YAP knockdown. Cell proliferation, colony formation, and IL-33, TSLP, and IL-25 mRNA expression were also decreased (Fig. 5A–C). The data demonstrated that inhibition of the hippo pathway by VP or lentiviral transfection could suppress the NF-κB pathway and epithelium-derived factor expression in RPMI 2650 cells.

3.5 YAP induced epithelium-derived cytokine expression via NF-κB signalling in epithelial cells derived from nasal polyp tissues

We used epithelial cells derived from nasal polyp tissues to confirm our results. We found that 2.5 μM VP effectively hampered hippo-YAP signalling (Fig. 6A). VP inhibited the expression of NF-κB and the proliferation of epithelial cells derived from nasal polyp tissues (Fig. 6B–F). Moreover, the mRNA levels of TSLP, IL-33, and IL-25 were significantly downregulated compared with those of normal control tissues (Fig. 6H–J). Furthermore, BAY 11-7082, a small molecule inhibitor of the NF-κB pathway, was employed to confirm the expression of VP-induced epithelium-derived factors. After treating NPECs with BAY 11-7082 for 24 h, the protein levels of pIκBα and NF-κB were attenuated significantly (Fig. 6K-L). Following treatment with 5 μM BAY 11-7082 for 24 h, the mRNA levels of TSLP, IL-33, and IL-25 were decreased accordingly (Fig. 6M–O), suggesting that the decreased levels of TSLP, IL-33, and IL-25 with inhibition of YAP were mediated by NF-κB suppression.

4 Discussion

Thus far, the molecular mechanisms contributing to the pathogenesis of nasal polyps, is still unclear. In our previously published study, we provided evidence that the hippo pathway, especially its core effector YAP, played a key role in upregulating nasal epithelial proliferation and remodelling in nasal polyps, which suggested the hippo pathway could be a valuable therapeutic target in nasal polyps.. However, how the hippo pathway regulates the pro-inflammatory effect of epithelial cells is still unknown. Thus, to uncover key insights of the control of hyper-inflammatory responses elicited from epithelial cells in CRSwNP, we identified possible pathway in epithelial proliferation and epithelium-derived innate cytokines production. Previously, it was shown that YAP protein level was positively correlated with epithelial basement membrane thickness and the Ki-67 mRNA level, and negatively correlated with the E-cadherin mRNA level in both eosinophilic and non-eosinophilic nasal polyps (Deng et al., 2019). Here, we found that YAP overexpression induced the upregulation of the epithelium-derived innate cytokines TSLP, IL-33, and IL-25 via NF-κB signalling, consistent with other studies that showed that NF-κB plays an important role in CRS (Kim, 2019). These novel findings provide new insights into the pathophysiology of inflammation in nasal polyps.

CRSwNP was heterogeneous and marked by niches of denuded respiratory epithelium with associated proliferation, basal membrane thickening, and goblet cell hyperplasia (Li et al., 2011; Li et al., 2014). In this study, it showed that aberrant expression of YAP induced epithelial cell proliferation during nasal polyp development. Moreover, when the hippo pathway in RPMI 2650 cells was downregulated, we found that the cells were arrested in G1 phase resulting in repressed cell growth. The cell cycle progression proteins cyclin D1 and CDK4 were also decreased when the hippo pathway was downregulated. Consistent with our findings, previous study found that YAP-deficient retinal progenitors displayed decreased S-phase cells and altered cell cycle progression (Kim et al., 2016). Furthermore, another study demonstrated that when YAP was decreased in cells from clear cell renal cell carcinoma, cell proliferation was inhibited (G1 phase arrest) and apoptosis was increased (Cao et al., 2014). In our study, however, VP regulation of the hippo pathway showed no effect on cell apoptosis. Future studies are still needed to further address its possible mechanism.

As previously reported, the nasal epithelium contributes to host defence and forms the physical barrier (Shah et al., 2016; Steelant et al., 2016), which served as the first line of defense of nose. In order to maintain the stable balance, airway epithelial cells plays a key role, which are characterised by innate and adaptive immunity, and produce a series of pro-inflammatory cytokines such as TSLP, IL-25, and IL-33 that orchestrate type 2 responses at the mucosa site (Lloyd and Saglani, 2015; Zheng et al., 2018). IL-33 and TSLP mRNA levels were increased in polyp tissues (Hong et al., 2018). In this study, we revealed that nasal polyp tissue had increased mRNA levels of the epithelium-derived innate cytokines TSLP, IL-25, and IL-33 compared with nasal tissue from healthy subjects. Much of the literature suggests that cytokines are involved in the pathogenesis of chronic nasal sinusitis or nasal polyps. However, the mechanism by which cytokine expression is upregulated has not been well documented. Several studies have demonstrated that the NF-κB pathway is highly activated in inflammatory disorders due to its ability to induce transcription of pro-inflammatory genes (Tak and Firestein, 2001; Yamamoto and Gaynor, 2001). In addition, the NF-κB pathway plays a critical role in host defence against pathogens, and protects cells

from apoptosis. When inactive, NF-κB exists as a heterodimer in the cytoplasm and binds inhibitor-kappa B (IκB). When the cells are subjected to various stimuli, such as inflammation, IκB is dephosphorylated and dissociates from NF-κB, of which the most important are IκBα, IκBβ, and IκBε. Similar to another study (Jung et al., 2019), we found that NF-κB activity involved in the production of epithelium-derived innate cytokines TSLP and IL-33, as well as IL-25 expression in epithelia cells from nasal polyps. Possibly, when an inflammatory process is initiated in nasal polyps, activated NF-κB translocates to the cell nucleus, inducing transcription, particularly of genes encoding inflammatory cytokines, chemokines, and adhesion molecules, such as TSLP, IL-33, and IL-25. This NF-κB-driven effect was further verified in a pharmacological inhibition experiment that showed that nasal polyp epithelial cells treated with BAY 11-7082 (5 μM). The mRNA levels of TSLP, IL-33, and IL-25 were decreased accordingly. Except for epithelial-derived cytokines, multiple inflammatory cytokines were highly expressed during NF-κB activation, such as tumour necrosis factor-α, IL-1β, and IL-6 (Youn et al., 2016; Kim et al., 2018), together indicating that the NF-κB pathway might involved in the pro-inflammation process in epithelial cells.

YAP functions as a transcriptional regulator by acting together with sequence-specific DNA binding factors and transcription cofactors to mediate cell proliferation in developing epithelial tissues and tumours. Our previous data demonstrated that YAP promoted epithelia cell proliferation (Deng et al., 2019). Meanwhile, it has been reported that NF-κB and NF-κB-related inflammatory cytokines are increased in nasal polyps, indicating that NF-κB has a pivotal role in the pathogenesis of CRSwNPs in both Caucasians and Asians (Jung et al., 2019). In the present study, we found that inhibition of YAP could reducethe NF-κB pathway. The interaction was supported by two studies. One study underscores the importance of the YAP1/TAZ–NFκB signaling axis in endodermal organ development and disease, and they found that Hippo suppresses NF-κB signaling in pancreatic progenitors to permit cell differentiation and epithelial morphogenesis (Braitsch et al., 2019). Besides, other researchers found that YAP enhances NF-κB-dependent and independent effects on clock-mediated unfolded protein responses and autophagy in sarcoma (Rivera-Reyes et al., 2018). Similarly, in our study, NPECs were treated with BAY 11-7082 (an inhibitor of IκB phosphorylation) to explore the levels of TSLP, IL-33, and IL-25. It was confirmed that YAP-induced upregulation of TSLP, IL-33, and IL-25 expression could be abrogated by NF-κB inhibition, indicating that YAP could induce TSLP, IL-33, and IL-25 expression in nasal epithelial cells via activation of the NF-κB pathway. Maybe VP is a potential treatment for inhibition of inflammation in nasal polyps by downregulating NF-κB signaling pathway. Further studies are warranted to characterize the roles of YAP and other hippo pathway components in the regulation of NF-κB pathway and cytokine expression in NP. Nevertheless, there are some other interesting foundings for the hippo/YAP-NFκB signaling axis. One study showed that TAK1 mediated YAP phosphorylation, resulting in a reciprocal antagonism between Hippo-YAP/TAZ and NF-κB signalling during osteoarthritis pathogenesis (Deng et al., 2018). The other study showed that TAK1 regulated YAP-derived oncogenicity in pancreatic cancer (Santoro et al., 2020). Further studies are warranted to characterize the exact regulated mechanism of YAP and NF-κB in the regulation of inflammatory cell functions in nasal polyps to find out if there was a bi-directional control mechanism.

In summary, we found that hippo/YAP promoted nasal epithelial cell proliferation and inhibition of YAP could downregulate the expression of TSLP, IL-33, and IL-25 via the NF-κB signaling pathway in nasal epithelial cells. Inhibition of the YAP pathway reduced cell proliferation and epithelial inflammation in nasal polyps, which serves as a potential therapeutic approach for treating nasal inflammation.

Declarations

Conflict of interest

The authors declare that the research was conducted in the absence of any commercial or financial relationships that could be construed as a potential conflict of interest.

Acknowledgements

The authors would like to thank all the patients for their participation in this study, as well as the funding, and the Third Affiliated Hospital, Sun Yat-Sen University.

Funding

This work was supported by the National Natural Science Foundation of China (Grant No. 81670912 and 81870704) and The Third Affiliated Hospital of Sun Yat-Sen University, Clinical Research Program (No. QHJH201901).

Consent for publication

Not applicable.

Ethics approval and consent to participate

All patients were informed of the purposes and procedures of the study and provided written informed consent. This study was approved by the Ethics Committee for Human Study at the Third Affiliated Hospital of Sun Yat-sen University (China).

Author contributions

All authors were involved in the study. Study conception and design: QY, ZL, ML and HD. Patient consent and enrollment: HD, ML and R Zh. Surgery: XH and HD. Acquisition of data or analysis and interpretation of data: HD, ML, HQ, QY, TY, ZL and RZh. Quality control of the study: XH and ZL. Drafting the article: HD, ML and RZh. Revising the article critically for important intellectual content and final approval of the version to be published: all authors.

Availability of data and materials

The dataset generated and analyzed during the current study are not publicly available due to data protection but are available from the corresponding author on reasonable request (excluding personal

data).

References

1. Braitsch CM, Azizoglu DB, Htike Y, Barlow HR, Schnell U, Chaney CP, et al. LATS1/2 suppress NFκB and aberrant EMT initiation to permit pancreatic progenitor differentiation. PLOS Biology. 2019;17(7):e3000382. doi:10.1371/journal.pbio.3000382.
2. Cao JJ, Zhao XM, Wang DL, Chen KH, Sheng X, Li WB, et al. YAP is overexpressed in clear cell renal cell carcinoma and its knockdown reduces cell proliferation and induces cell cycle arrest and apoptosis. Oncol Rep. 2014;32(4):1594–600. doi:10.3892/or.2014.3349.
3. Chen X, Chang L, Li X, Huang J, Yang L, Lai X, et al. Tc17/IL-17A Up-Regulated the Expression of MMP-9 via NF-kappaB Pathway in Nasal Epithelial Cells of Patients With Chronic Rhinosinusitis. Front Immunol. 2018;9:2121. doi:10.3389/fimmu.2018.02121.
4. Deng H, Sun Y, Wang W, Li M, Yuan T, Kong W, et al. The hippo pathway effector Yes-associated protein promotes epithelial proliferation and remodeling in chronic rhinosinusitis with nasal polyps. Allergy. 2019;74(4):731–42. doi:10.1111/all.13647.
5. Deng Y, Lu J, Li W, Wu A, Zhang X, Tong W, et al. (2018). Reciprocal inhibition of YAP/TAZ and NF-κB regulates osteoarthritic cartilage degradation. Nat Commun 9(1). doi:10.1038/s41467-018-07022-2.
6. Fokkens WJ, Lund VJ, Mullol J, Bachert C, Alobid I, Baroody F, et al. European Position Paper on Rhinosinusitis and Nasal Polyps 2012. Rhinol Suppl. 2012;23(3):1–298. doi.
7. Halder G, Johnson RL. Hippo signaling: growth control and beyond. Development. 2011;138(1):9–22. doi:10.1242/dev.045500.
8. Hong HY, Chen FH, Sun YQ, Hu XT, Wei Y, Fan YP, et al. Local IL-25 contributes to Th2-biased inflammatory profiles in nasal polyps. Allergy. 2018;73(2):459–69. doi:10.1111/all.13267.
9. Hupin C, Gohy S, Bouzin C, Lecocq M, Polette M, Pilette C. Features of mesenchymal transition in the airway epithelium from chronic rhinosinusitis. Allergy. 2014;69(11):1540–9. doi:10.1111/all.12503.
10. Johnson RL. Hippo signaling and epithelial cell plasticity in mammalian liver development, homeostasis, injury and disease. Sci China Life Sci. 2019;62(12):1609–16. doi:10.1007/s11427-018-9510-3.
11. Jung HJ, Zhang YL, Kim DK, Rhee CS, Kim DY. The Role of NF-kappaB in Chronic Rhinosinusitis With Nasal Polyps. Allergy Asthma Immunol Res. 2019;11(6):806–17. doi:10.4168/aair.2019.11.6.806.
12. Kim DO, Byun JE, Seong HA, Yoon SR, Choi I, Jung H. Thioredoxin-interacting protein-derived peptide (TN13) inhibits LPS-induced inflammation by inhibiting p38 MAPK signaling. Biochem Biophys Res Commun. 2018;507(1–4):489–95. doi:10.1016/j.bbrc.2018.11.069.
13. Kim JY, Park R, Lee JH, Shin J, Nickas J, Kim S, et al. Yap is essential for retinal progenitor cell cycle progression and RPE cell fate acquisition in the developing mouse eye. Dev Biol. 2016;419(2):336–47. doi:10.1016/j.ydbio.2016.09.001.

14. Kim YH. Establishing a Therapeutic Strategy Targeting NF-kappaB in Asian Patients with Chronic Rhinosinusitis With Nasal Polyps. Allergy Asthma Immunol Res. 2019;11(6):757–9. doi:10.4168/aair.2019.11.6.757.
15. Lange AW, Sridharan A, Xu Y, Stripp BR, Perl AK, Whitsett JA. Hippo/Yap signaling controls epithelial progenitor cell proliferation and differentiation in the embryonic and adult lung. J Mol Cell Biol. 2015;7(1):35–47. doi:10.1093/jmcb/mju046.
16. Li CW, Shi L, Zhang KK, Li TY, Lin ZB, Lim MK, et al. Role of p63/p73 in epithelial remodeling and their response to steroid treatment in nasal polyposis. J Allergy Clin Immunol. 2011;127(3):765–72. doi:10.1016/j.jaci.2010.12.011.
17. Li YY, Li CW, Chao SS, Yu FG, Yu XM, Liu J, et al. Impairment of cilia architecture and ciliogenesis in hyperplastic nasal epithelium from nasal polyps. J Allergy Clin Immunol. 2014;134(6):1282–92. doi:10.1016/j.jaci.2014.07.038.
18. Lloyd CM, Saglani S. Epithelial cytokines and pulmonary allergic inflammation. Curr Opin Immunol. 2015;34:52–8. doi:10.1016/j.coi.2015.02.001.
19. Mitani A, Nagase T, Fukuchi K, Aburatani H, Makita R, Kurihara H. Transcriptional coactivator with PDZ-binding motif is essential for normal alveolarization in mice. Am J Respir Crit Care Med. 2009;180(4):326–38. doi:10.1164/rccm.200812-1827OC.
20. Mjosberg JM, Trifari S, Crellin NK, Peters CP, van Drunen CM, Piet B, et al. Human IL-25- and IL-33-responsive type 2 innate lymphoid cells are defined by expression of CRTH2 and CD161. Nat Immunol. 2011;12(11):1055–62. doi:10.1038/ni.2104.
21. Rivera-Reyes A, Ye S, E MG, Egolf S, E, C.G., and Chor S, et al. YAP1 enhances NF-kappaB-dependent and independent effects on clock-mediated unfolded protein responses and autophagy in sarcoma. Cell Death Dis. 2018;9(11):1108. doi:10.1038/s41419-018-1142-4.
22. Santoro R, Zanotto M, Simionato F, Zecchetto C, Merz V, Cavallini C, et al. Modulating TAK1 Expression Inhibits YAP and TAZ Oncogenic Functions in Pancreatic Cancer. Mol Cancer Ther. 2020;19(1):247–57. doi:10.1158/1535-7163.MCT-19-0270.
23. Shah SA, Ishinaga H, Takeuchi K. (2016). Pathogenesis of eosinophilic chronic rhinosinusitis. J Inflamm 13(1). doi:10.1186/s12950-016-0121-8.
24. Shi JB, Fu QL, Zhang H, Cheng L, Wang YJ, Zhu DD, et al. Epidemiology of chronic rhinosinusitis: results from a cross-sectional survey in seven Chinese cities. Allergy. 2015;70(5):533–9. doi:10.1111/all.12577.
25. Steelant B, Seys SF, Boeckxstaens G, Akdis CA, Ceuppens JL, Hellings PW. Restoring airway epithelial barrier dysfunction: a new therapeutic challenge in allergic airway disease. Rhinology. 2016;54(3):195–205. doi:10.4193/Rhin15.376.
26. Stevens WW, Lee RJ, Schleimer RP, Cohen NA. Chronic rhinosinusitis pathogenesis. J Allergy Clin Immunol. 2015;136(6):1442–53. doi:10.1016/j.jaci.2015.10.009.
27. Tak PP, Firestein GS. NF-kappaB: a key role in inflammatory diseases. J Clin Invest. 2001;107(1):7–11. doi:10.1172/JCI11830.

28. Van Bruaene N, Van Crombruggen CPN, De Ruyck K, Holtappels N, G., and Van Cauwenberge P, et al. Inflammation and remodelling patterns in early stage chronic rhinosinusitis. Clin Exp Allergy. 2012;42(6):883–90. doi:10.1111/j.1365-2222.2011.03898.x.
29. Watelet JB, Van Zele T, Gjomarkaj M, Canonica GW, Dahlen SE, Fokkens W, et al. Tissue remodelling in upper airways: where is the link with lower airway. remodelling? Allergy. 2006;61(11):1249–58. doi:10.1111/j.1398-9995.2006.01226.x.
30. Xu R, Xu G, Shi J, Wen W. A correlative study of NF-kappaB activity and cytokines expression in human chronic nasal sinusitis. J Laryngol Otol. 2007;121(7):644–9. doi:10.1017/S0022215106001824.
31. Yamamoto Y, Gaynor RB. Therapeutic potential of inhibition of the NF-kappaB pathway in the treatment of inflammation and cancer. J Clin Invest. 2001;107(2):135–42. doi:10.1172/JCI11914.
32. Yan Y, Gordon WM, Wang DY. Nasal epithelial repair and remodeling in physical injury, infection, and inflammatory diseases. Curr Opin Otolaryngol Head Neck Surg. 2013;21(3):263–70. doi:10.1097/MOO.0b013e32835f80a0.
33. Youn GS, Lee KW, Choi SY, Park J. Overexpression of HDAC6 induces pro-inflammatory responses by regulating ROS-MAPK-NF-kappaB/AP-1 signaling pathways in macrophages. Free Radic Biol Med. 2016;97:14–23. doi:10.1016/j.freeradbiomed.2016.05.014.
34. Yu FX, Zhao B, Guan KL. Hippo Pathway in Organ Size Control, Tissue Homeostasis, and Cancer. Cell. 2015;163(4):811–28. doi:10.1016/j.cell.2015.10.044.
35. Zhang GC, Yu XN, Sun JL, Xiong J, Yang YJ, Jiang XM, et al. UBE2M promotes cell proliferation via the beta-catenin/cyclin D1 signaling in hepatocellular carcinoma. Aging. 2020;12(3):2373–92. doi:10.18632/aging.102749.
36. Zhao B, Tumaneng K, Guan KL. The Hippo pathway in organ size control, tissue regeneration and stem cell self-renewal. Nat Cell Biol. 2011;13(8):877–83. doi:10.1038/ncb2303.
37. Zhao R, Fallon TR, Saladi SV, Pardo-Saganta A, Villoria J, Mou H, et al. Yap tunes airway epithelial size and architecture by regulating the identity, maintenance, and self-renewal of stem cells. Dev Cell. 2014;30(2):151–65. doi:10.1016/j.devcel.2014.06.004.
38. Zheng R, Wang D, Wang K, Gao WX, Yang QT, Jiang LJ, et al. Elevated expression of IL-17RB and ST2 on myeloid dendritic cells is associated with a Th2-skewed eosinophilic inflammation in nasal polyps. Clin Transl Allergy. 2018;8:50. doi:10.1186/s13601-018-0237-4.

Figures

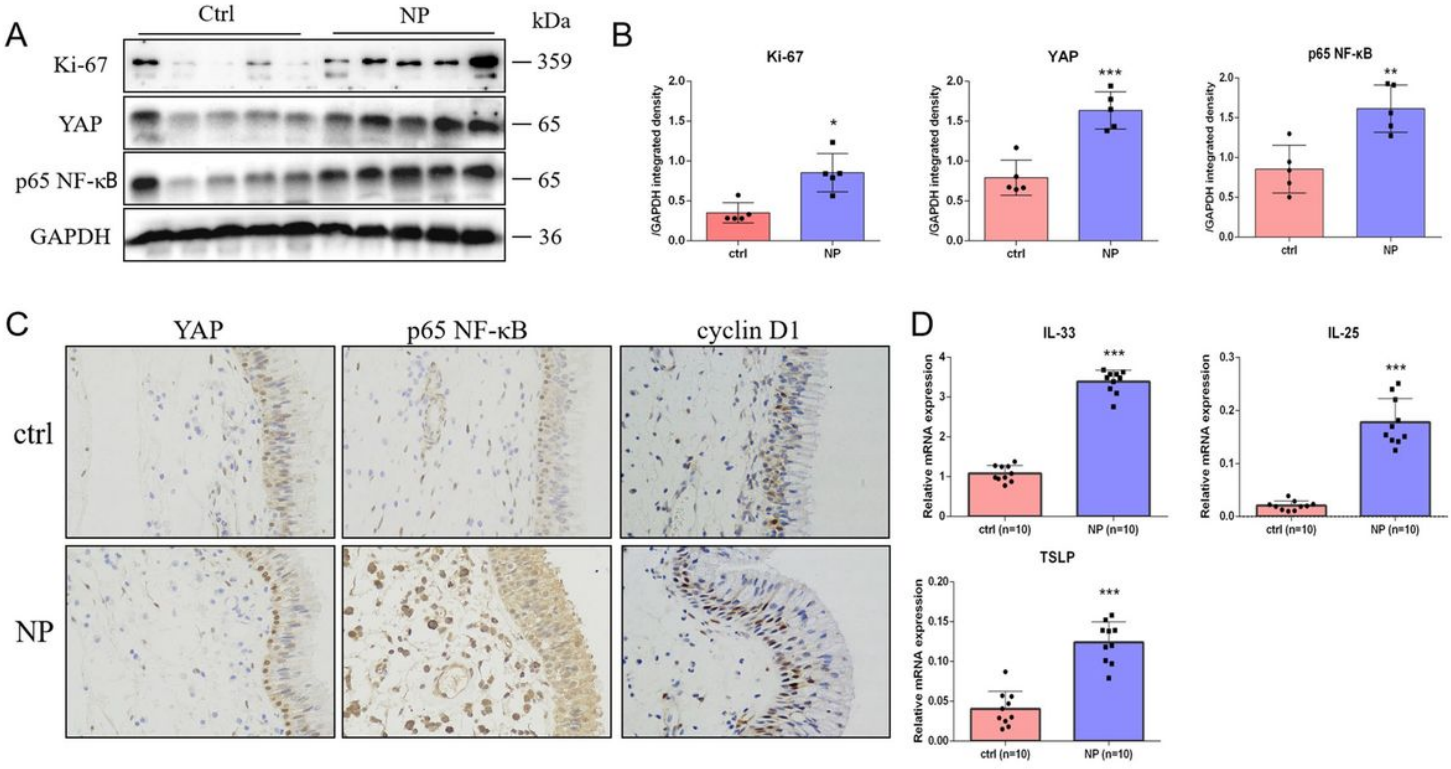

Figure 1

Expression of hippo pathway effector YAP, NF-κB and epithelium-derived factor in healthy controls and nasal polyps. (A-B) Western blotting analysis for YAP, Ki-67, p65 NF-κB and GAPDH expression in total protein extracted from nasal tissues. Representative images from each group are shown. All the bands on the panels were quantified by densitometric analysis using Image J software, and data were expressed as relative values against GAPDH (n = 5 for each group, Independent-Sample t test). (C) Immunohistochemical staining for YAP in polyp tissues and healthy control tissues. Representative images from each group are shown (n = 10 for each group, 400×magnification). (D) Quantitative analysis of transcript levels of epithelium-derived factor including TSLP, IL-33 and IL-25 relative to the expression level of β2 microglobulin (β2M) reference gene in nasal polyp tissues as well as healthy control tissues (n = 10 for each group, Mann-Whitney U 2-test). Data are presented as mean ± SD. * $P < 0.05$, ** $P < 0.01$, *** $P < 0.001$.

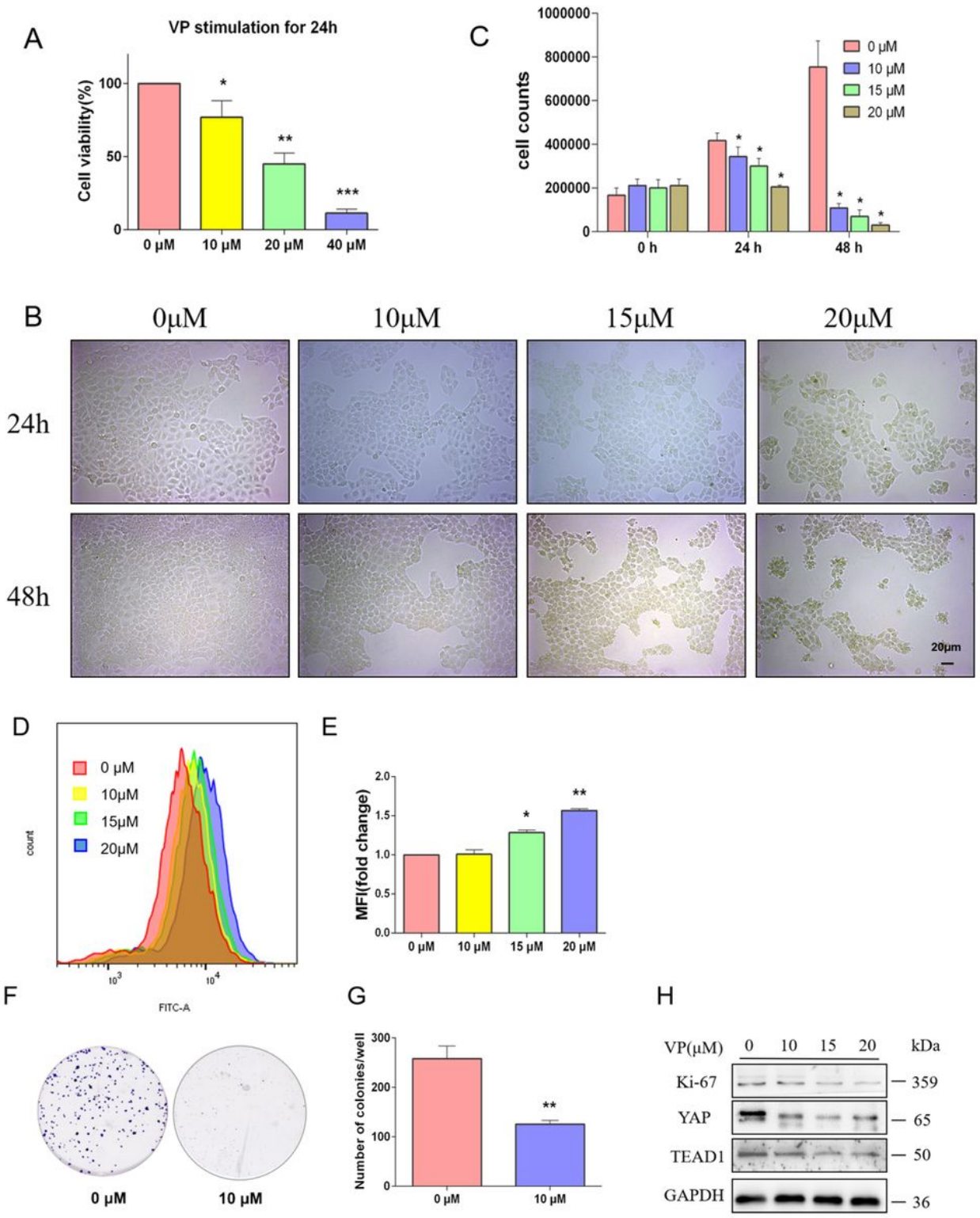

Figure 2

Pharmaceutical inhibition of hippo pathway activity suppresses cell proliferation of RPMI 2650 cells. (A) Cell growth curve showed the cell viability of RPMI 2650 cells treated with verteporfin treatment for 24 h in different density gradient via CCK-8 assay. (B) RPMI 2650 cells were incubated under verteporfin treatment for 24 and 48 h in different density gradient. Morphologic change was photographed at 200× magnification (n= 3 for each group).. (C) Cell count was measured in cells treated with verteporfin (0, 10,

15, 20 μM) using trypan blue stain assay (n = 3 for each group, one-way ANOVA). (D-E) CFSE cytometric analysis of cell proliferation after VP treatment for 24 h in various density gradient (n = 3 for each group). Quantification of mean fluorescence intensity (MF) in different group (n = 3 for each group, one-way ANOVA). (F-G) The ability of proliferation was measured by plate colony-forming assay. Representative images from each group are shown by scanner. The cell counting was measured by counting clone number growing in plate using Image J software (n = 3 for each group, Independent-Sample t test). (H) Protein levels of YAP, TEAD1 and Ki-67 were detected in RPMI 2650 cells treated with verteporfin for 24 h (n= 3 for each group).. Results are the mean ± SD. *P < 0.05, ** P < 0.01, *** P < 0.001.

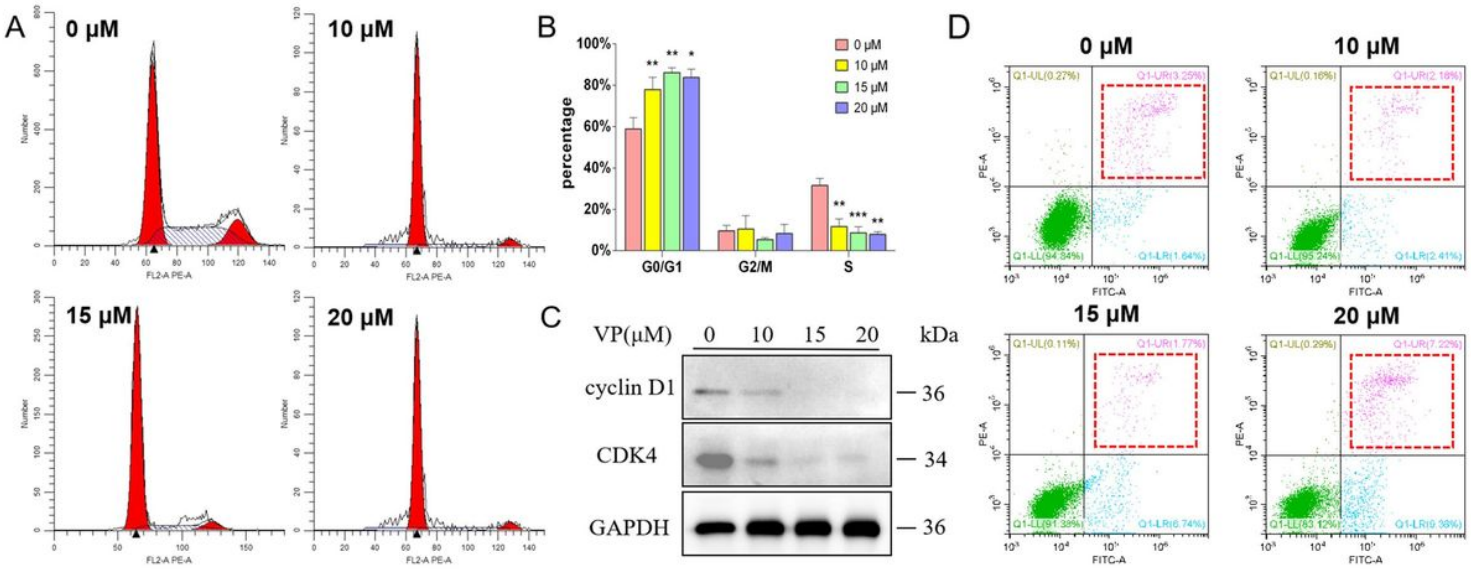

Figure 3

Inhibition of YAP induces cell cycle arrest in RPMI 2650 cells. (A) The apoptosis assay of the cell cycle of RPMI 2650 cells treated with VP (0, 10, 15,20 μM) after 24 h. (B) The proportion of cells in each phase was shown (n = 3 for each group, one-way ANOVA). (C) Representative western blotting analysis of cell cycle progression proteins cyclinD1 and CDK4 in RPMI 2650 cells treated with VP for 24 h (n= 3 for each group). (D) RPMI 2650 cells were treated with VP for 24 h and the apoptosis was detected (n= 3 for each group). Data were presented as mean ± SD. * P < 0.05, ** P < 0.01, *** P < 0.001.

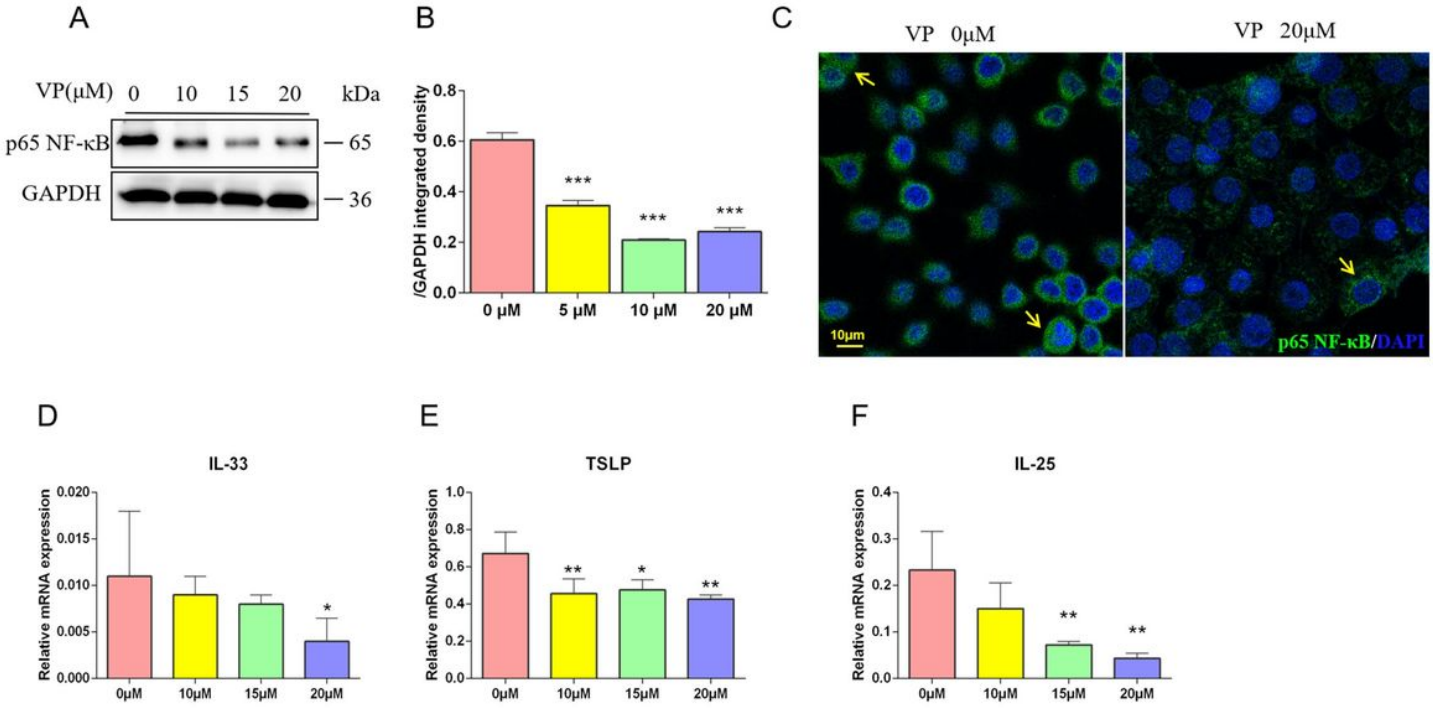

Figure 4

Pharmaceutical inhibition of hippo pathway activity suppresses NF-κB pathway and epithelium-derived factor expression in RPMI 2650 cell. (A-B) Western blotting analysis p65 NF-κB after cells were treated with VP for 24 h (n= 3). (C) The confocal sections of RPMI 2650 cells immunostained with rabbit anti-p65 NF-κB and DAPI. Representative confocal images from each group are shown (n = 3 for each group, 630×magnification). (D-F) Quantitative analysis of transcript levels of and epithelium-derived factor including TSLP, IL-33 and IL-25 in RPMI 2650 cells (n = 3 for each group, Kruskal-Wallis H-test). Data are presented as mean ± SD. * P < 0.05, ** P < 0.01.

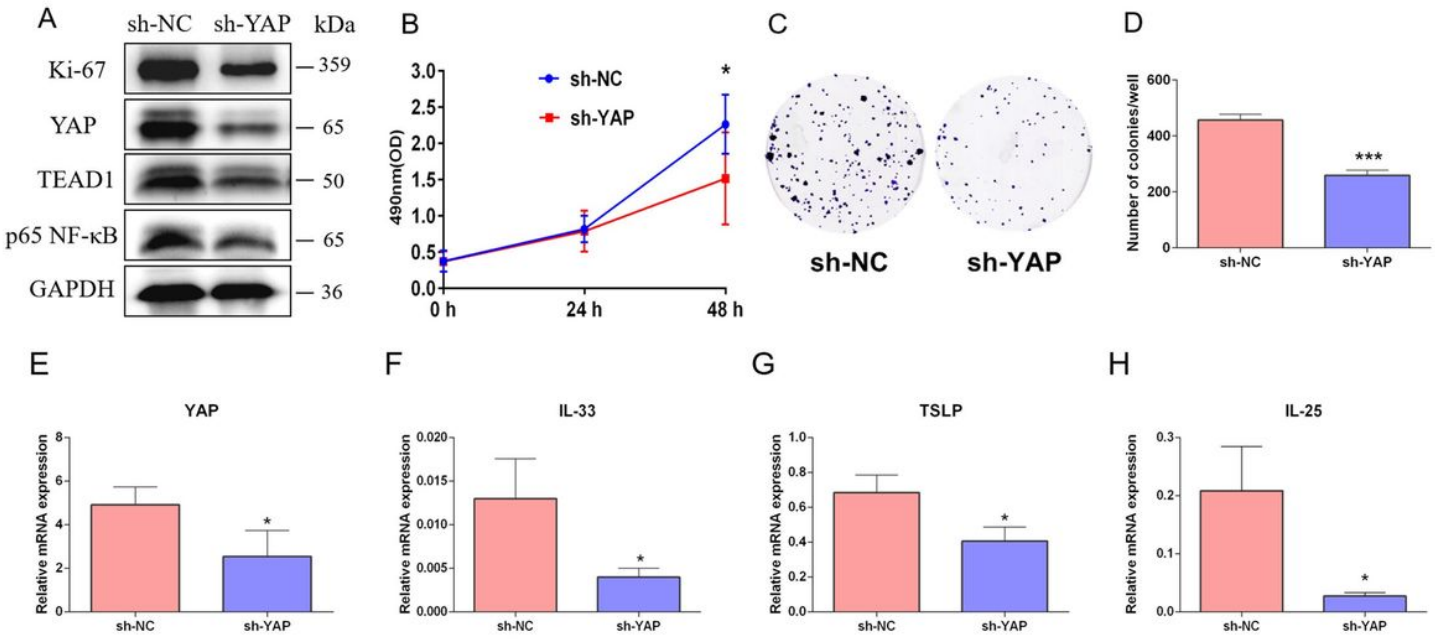

Figure 5

Lentiviral transfection mediated knockdown of YAP results in suppression of cell proliferation properties, and decreased expression of epithelium-derived factors. (A) Protein levels of Ki-67, YAP, TEAD1 and p65 NF-κB in YAP knockdown cells (n=3). (B) CCK-8 assay was used to evaluate the effect of YAP knockdown on cell proliferation of RPMI 2650 cells after 24 and 48 h (n=3 for each group, Independent-Sample t Test). (C-D) The ability of cell proliferation was measured by colony-forming assay. Representative images from each group are shown (n = 3 for each group, Independent-Sample t Test). (E-H) YAP, TSLP, IL-33 and IL-25 mRNA levels by RT- PCR in RPMI 2650 cells (n=3 for each group, Mann–Whitney U 2-test). Data are presented as mean ± SD. * $P < 0.05$, *** $P < 0.001$.

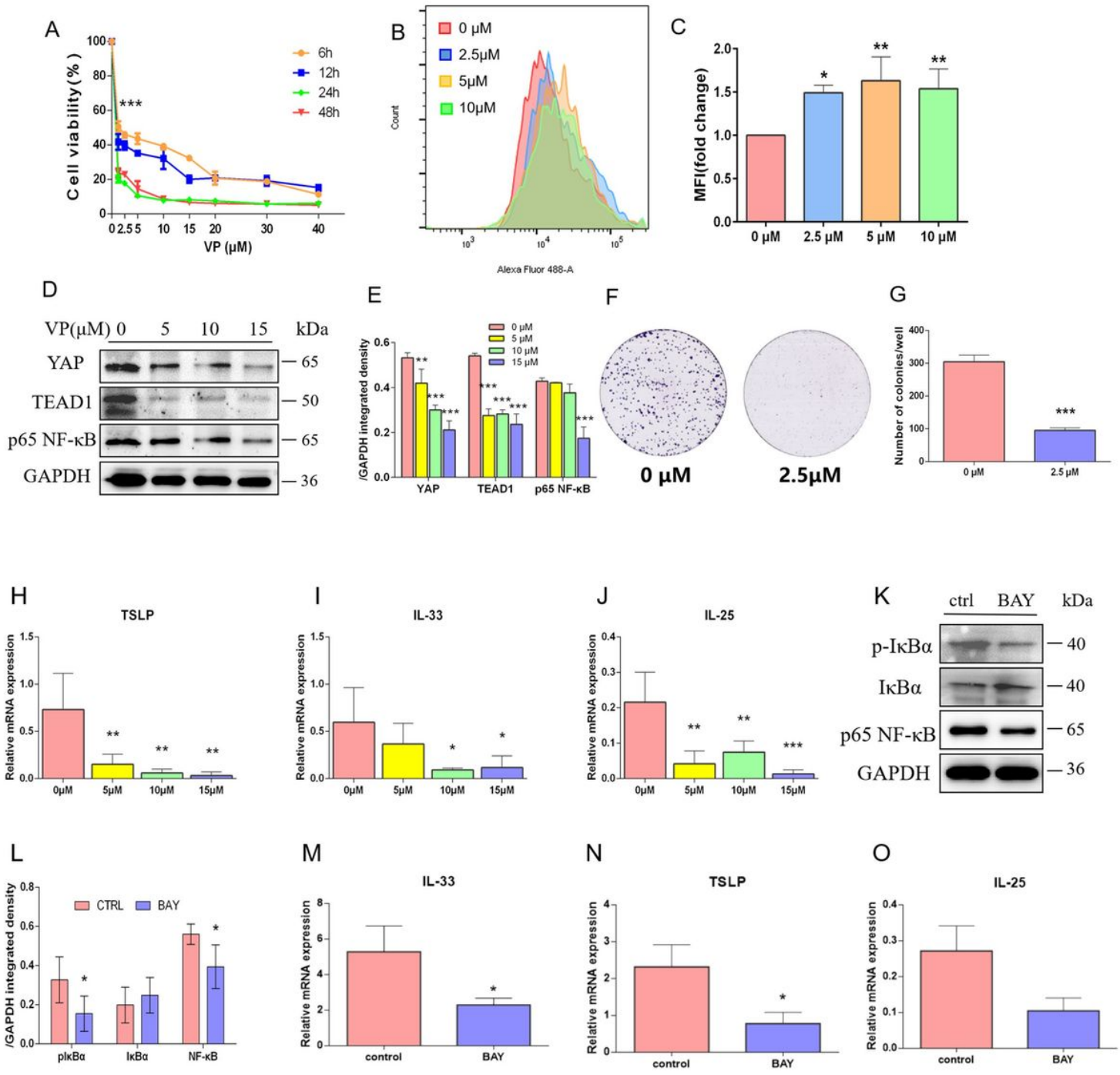

Figure 6

Suppression of cell proliferation by inhibition of YAP was mediated by NF-κB. (A) CCK-8 assay showed the cell viability of NPECs treated with verteporfin from 6 h to 48 h in different density gradient (0μM-40μM), respectively (n=3). (B-C) Flow cytometry of cell proliferation with VP treatment in human nasal polyps. The cells were cultured with VP for 24 h after CFSE staining. Quantification of MF in various conditions was shown. (n = 3 for each group, one-way ANOVA). (D-E) Quantification of YAP, TEAD1 and p65 NF-κB expression after stimulation with VP for 24 h by Image J software (n = 3 for each group, one-

way ANOVA). (F-G) The biological behavior changes of the NPECs were observed by colony formation assay. Representative images from each group are shown (n = 3 for each group, Independent-Sample t Test). (H-J) Quantitative analysis of mRNA levels of TSLP, IL-33 and IL-25 from primary nasal polyp epithelial cells treated with VP for 24 h (n = 3, Kruskal-Wallis H-test). (K-L) NPECs was incubated with BAY (5μM) for 24 h. Werstern blotting was performed to measure the expression of the key protein levels of NF-κB pathway (n = 3). (M-O) The mRNA expression levels of TSLP, IL-33 and IL-25 were detected relative to the expression level of β2M in NPECs incubated with or without BAY (5μM) for 24 h (n = 3, Mann–Whitney U 2-test). Results are the mean ± SD. * $P < 0.05$, ** $P < 0.01$, *** $P < 0.001$.